Advanced glycation end-products promote hepatosteatosis by interfering with SCAP-SREBP pathway in fructose drinking mice

Advanced glycation end-products promote hepatosteatosis by interfering with SCAP-SREBP pathway in fructose drinking mice

Raffaella Mastrocola[1], PhD, Massimo Collino[2], PhD, Mara Rogazzo[2], PhD student, Claudio Medana[3], PhD, Debora Nigro[1], PhD student, Giuseppe Boccuzzi[4], MD, Manuela Aragno[1], PhD.

Affiliations: [1]Department of Clinical and Biological Sciences, Experimental Medicine and Clinical Pathology Unit, University of Turin, Italy; [2]Department of Drug Science and Technology, University of Turin, Turin, Italy; [3]Department of Molecular Biotechnology and Life Sciences, University of Turin, Italy; [4]Oncological Endocrinology, University of Turin, Italy.

Author contribution: experiments planning and manuscript drafting: RM, MA, and GB; animal treatment: RM and MC; analytical chemistry studies: CM; biochemical parameters detection and biomolecular techniques: DN and MR.

Corresponding author:
Raffaella Mastrocola, PhD
Dept. of Clinical and Biological Sciences
Experimental Medicine and Clinical Pathology Unit
University of Turin - C.so Raffaello 30 - 10125 Torino, Italy
Tel: +390116707758 - Fax: +390116707753
E-mail address: raffaella.mastrocola@unito.it

Running head title: AGEs induce SREBP1c activation

Abstract

Clinical studies have linked the increased consumption of fructose to the development of obesity, dyslipidemia and impaired glucose tolerance, and a role in hepatosteatosis development is presumed. Fructose can undergo a non-enzymatic reaction from which advanced glycation endproducts (AGEs) are derived, leading to the formation of dysfunctional, fructosylated proteins, however the *in vivo* formation of AGEs from fructose is still less known than that from glucose.

In the present study C57Bl/6J mice received 15% (w/v) fructose (FRT) or 15% (w/v) glucose (GLC) in water to drink for 30 weeks, resembling human habit to consume sugary drinks. At the end of protocol both FRT and GLC drinking mice had increased fasting glycaemia, glucose intolerance, altered plasma lipid profile, and marked hepatosteatosis. FRT mice had higher hepatic triglycerides deposition than GLC, paralleled by a greater increased expression and activity of the sterol regulatory element-binding protein 1 (SREBP1), the transcription factor responsible for the *de novo* lipogenesis, and of its activating protein SCAP. LC-MS analysis showed a different pattern of AGEs production in liver tissue between FRT and GLC mice, with larger amount of carboxymethyl lysine (CML) generated by FRT. Double immunofluorescence and coimmunoprecipitation analysis revealed an interaction between CML and SCAP that could lead to prolonged activation of SREBP1.

Overall, the high levels of CML and activation of SCAP/SREBP pathway associated to high fructose exposure here reported may suggest a key role of this signaling pathway in mediating fructose-induced lipogenesis.

Key words: AGEs; SREBP; triglyceride synthesis; soft drink; hepatosteatosis; fructose; glucose; carboxymethyl lysine.

Introduction

Many clinical studies have linked the rising consumption of soft drinks added with fructose to the development of obesity, dyslipidemia, insulin resistance, impaired glucose tolerance, and hypertension in adults (6,9,19, 26). Interestingly, clinical data show that inclusion of fructose in the diet for 10 weeks leads to a greater increase in hepatic lipid synthesis than that occurring with an equal amount of glucose (42).

Lipid metabolism is regulated by the sterol regulatory element binding proteins (SREBP) family, comprising three subtypes: SREBP-1a and SREBP-1c, which are generated by alternative splicing, and SREBP-2. SREBP-1c, expressed in most tissues with a greater prevalence than SREBP1a in liver and adrenal glands, is in charge of governing fatty acid and triacylglyceride metabolism, while SREBP-2, ubiquitously expressed, is involved in the regulation of cholesterol metabolism. Both SREBP-1 and SREBP-2 are synthesized as membrane proteins in the endoplasmic reticulum (ER) forming a complex with the SREBP-cleavage activating protein (SCAP). In spite of the distinct roles of the SREBPs in lipid metabolism, they are both subjected to the identical processing pathway (37): when TG or cholesterol synthesis are required, SCAP shuttles SREBPs from the endoplasmic reticulum (ER) to the Golgi, where they are cleaved by two proteases and enter the nucleus, bind to the sterol-regulatory elements in the promoters of target genes and increase transcription of lipogenic or cholesterologenic enzymes (17). Interestingly, SREBP-1 and SREBP-2 processing is triggered by different types of stimuli: while SREBP-1 activation depends primarily on insulin signaling and nutritional status, SREBP-2 is sensitive to membrane sterols level (37).

The liver is the main organ in which fructose metabolism takes place rapidly leading to increased hepatic synthesis of glycogen, fatty acids and triglycerides (TG) (45). Nonalcoholic fatty liver disease (NAFLD) is the most common disorder in industrialized countries, affecting 15-20% of the general population (49) and epidemiological studies have indicated that the development of NAFLD may be associated with excessive fructose consumption (35,50).

Among the chemical properties of fructose, a non-enzymatic pathway known as the Maillard reaction is reported, in which fructose reacts with the aminic groups of proteins. After this reaction, the anomerisation equilibrium of fructose is displaced toward the open form of the sugar, which is highly reactive, especially compared to the forms derived from glucose (43). The Maillard reaction is also one of the "classic" pathways from which the advanced glycation endproducts (AGEs) are derived. It is known that a mixed class of toxic AGEs can be produced from the reduction of glucose (49): CML (carboxymethyl lysine) and pentosidine are obtained through an oxidative process, while MGO (methylglyoxal) and GLAP (glyceraldehyde-derived pyridinium compound) through a non-oxidative process. Additionally, glucose is known to form AGE alpha-oxoaldehydes, including GOLD (glyoxal-lysine dimer) and MOLD (methylglyoxal-lysine dimer), through the polyol pathway (41). AGEs can exert a direct interference with cellular proteins function or a receptor-mediated action, the latter being chiefly attributed to bonding with RAGE (Receptor for AGE) (4). The interaction between AGEs and RAGE leads to intracellular signals responsible for activation of pro-inflammatory transcription factors, such as NFkB (nuclear factor-kB) (3).

The Maillard reaction undertaken by fructose leads to the formation of altered, fructosylated proteins, which are potentially toxic, indicating that fructose, together with glucose, plays an important role in the formation of AGEs. So far, the *in vivo* formation of fructose-derived AGEs has only been demonstrated in one study, and only through immunochemical analysis, without reporting a description of their chemical structure (44). Thus, the chemical structure and toxicity of AGEs molecules specifically derived from fructose are less well known than those derived from glucose.

It might be hypothesized that the entrance of fructose in hepatocytes, where fructose is metabolized, leads to the fructosylation of cytoplasmic proteins, causing a loss of their functionality and regulation, thus contributing to liver alterations.

This study is aimed to characterized fructose-derived AGEs and to investigate their target proteins in liver by a comparative analysis between fructose and glucose-drinking mice.

Materials and Methods

All compounds were purchased from Sigma Chemical Co. (St. Louis, MO, USA) and all primary antibodies were from Santa Cruz Biotechnology (Santa Cruz, CA, USA), unless otherwise stated.

Animals and treatments

Male C57Bl6/N mice (Charles River Laboratories, Calco, LC, Italy) aged 5 weeks were cared for in compliance with the European Council directives (No. 86/609/EEC) and with the Principles of Laboratory Animal Care (NIH No. 85–23, revised 1985). The scientific project was approved by the local ethical committee. The animals were divided into three groups of 8-10 mice: CTRL-group, drinking tap water; FRT-group, drinking a 15% fructose solution; GLC-group, drinking a 15% glucose solution. All groups were fed with a standard lab chow and received drink and food *ad libitum*.

Body weight, drink and food intake were recorded weekly. Fasting glycemia was measured at the start of the protocol and every 8 weeks by saphenous vein puncture using a glucometer (GlucoGmeter, Menarini Diagnostics, Firenze, Italy). After 30 weeks mice were anesthetized and killed by cardiac exsanguination. Blood was collected and plasma isolated. The liver was rapidly removed. A portion was cryoprotected in OCT (Optimal Cutting Temperature) compound (VWR, Milano, Italy) and frozen in N_2 for cryostatic preparations. Other portions were frozen in N_2 and stored at −80°C for protein analysis.

Oral glucose tolerance test

Before killing, a glucose solution was administered orally at 2 g/kg b.w after a fasting period of 6 h. Plasma glucose levels were measured every 30 minutes for 2 hrs after glucose loading.

Biochemical parameters

Plasma lipid profile was determined by standard enzymatic procedures using reagent kits (triglycerides (TG), cholesterol, high-density lipoproteins (HDL), low-density lipoproteins (LDL): Hospitex Diagnostics, Florence, Italy; non-esterified fatty acid (NEFA): Wako Chemicals,Neuss, Germany).

Plasma insulin level was measured using an enzyme-linked immunosorbent assay (ELISA) kit (Mercodia AB, Uppsala, Sweden).

For tissue TG and cholesterol content determination, colorimetric assay kits were used after lipid extraction (TG: Triglyceride Quantification Kit, Abnova Corporation, Aachen, Germany; cholesterol: Hospitex Diagnostics).

Oil red staining

Liver lipid accumulation was evaluated by oil red staining on 4 μm cryostatic sections. Stained tissues were viewed under an Olympus Bx4I microscope (10x magnification) with an AxioCamMR5 photographic attachment (Zeiss, Gottingen, Germany). The sections were analyzed on six fileds/slide and scored by a blinded pathologist using the NAFLD activity score (NAS) system (21).

Preparation of tissue extracts

Liver cytosolic, nuclear, and total proteins were extracted as previously described (28). Protein content was determined using the Bradford assay and samples were stored at -80°C until use.

AGEs analysis with LC-MS

Pentosidine, GOLD, MOLD, CML, and GLAP, were evaluated on total liver extracts after hydrolisis with 0.6 M trichloroacetic acid and 50 μL of hydrochloric acid 6 M for 12 hours at 60°C. The chromatographic separations were run on an Ultimate 3000 HPLC (Dionex, Milan, Italy) coupled to a high resolving power mass spectrometer (HRMS) LTQ Orbitrap (Thermo Scientific, Rodano, Italy), equipped with an atmospheric pressure interface and an ESI ion source. The samples were analyzed using an Reverse Phase C18 column (Phenomenex Synergi 150 × 2.1 mm, 3 μm particle size) at a flow rate of 200 μL/min. A gradient mobile phase composition was adopted: 95/5 to 40/60 in 25 min, 5 mM heptafluorobutanoic acid/acetonitrile. The monitored protonated molecular ions were 205.1188 *m/z* for CML, 255.1344 *m/z* for GLAP, 341.2189 *m/z* for MOLD, 327.2032 *m/z* for GOLD and 379.2094 *m/z* for pentosidine. Quantitative determination of all the analytes were done by using pentosidine calibration data.

Western blotting.

Equal amounts of total, cytosolic or nuclear proteins were separated by SDS-PAGE and electrotransferred to nitrocellulose membrane (GE-Healthcare Europe, Milano, Italy). Mouse anti-NFkBp65, rabbit anti-SREBP1 and mouse anti-SREBP2 antibodies were probed on both cytosolic and nuclear extracts. Goat anti-ICAM-1 (intercellular adhesion molecule-1) and anti-CTGF (connective tissue growth factor), rabbit anti-SCAP, anti-ACC (Cell Signaling Technology, Danver, MA,USA), anti-HMGR (Millipore, Temecula, CA, USA), anti-apoB, anti-CPT1-L, and anti-RAGE were probed on total extracts. Rabbit anti-apoB was also probed on 10 ul of plasma samples.

Proteins were detected with ECL chemiluminescence substrate (GE-Healthcare) and quantified by densitometry using analytic software (Quantity-One, Bio-Rad). β-actin served as loading control for total and cytosolic protein extracts, and lamin-B1 for nuclear extracts.

Immunofluorescence

Localization of SCAP, SREBP1, CML and MGO was assessed on 4 μm liver cryostatic sections by indirect immunofluorescence. Sections were blocked for 1 h with 3% BSA in PBS added with unconjugated goat anti-mouse IgG to prevent mouse-on-mouse interferences. Thus, sections were incubated overnight with rabbit anti-SCAP, rabbit anti-SREBP1, mouse anti-CML (Trans-Genic, Kobe, Japan) or mouse anti-MGO (Trans-Genic) primary antibodies and for 1 h with fluorescent secondary antibodies (Dako, Glostrup, Denmark): TRITC-conjugated anti-rabbit IgG or biotin-conjugated anti-mouse IgG followed by FITC-conjugated streptavidin. Negative controls were prepared incubating sections with secondary antibodies. Sections were examined using a Leica Olympus epifluorescence microscope (Olympus Bx4I) and digitised with a high resolution camera (Zeiss).

Double immunofluorescence.

Double immunofluorescence was performed for SCAP and CML on liver cryostatic sections. After blocking, sections were incubated with a mix of primary antibodies for 1 hour. After washing, sections were incubated with a mix of labelled secondary antibodies. The images were colour-

combined and assembled into photomontages by using Adobe Photoshop (Universal Imaging, West Chester, PA).

Co-immunoprecipitation.

Equal amounts of total proteins (500 μg) were incubated overnight with SCAP rabbit-polyclonal antibody (2 μg). The antibody-antigen complexes were then incubated with fresh Protein A Sepharose beads for 3 h. SDS Laemmli buffer was added to the beads and eluted proteins were subjected to SDS–PAGE and immunoblotted with mouse anti-CML monoclonal antibody and, after stripping, with rabbit anti-SCAP antibody.

Statistical analysis

All values are expressed as means ± SD and were analyzed by Anova test followed by Bonferroni's post-test. A P value <0.05 was considered statistically significant.

Results

Fructose and glucose drinking in mice induces alterations in body weight, glucose tolerance and plasma lipid profile.

The daily drink intake in the FRT and GLC drinking groups was markedly higher than in the CTRL group, drinking tap water. Moreover, GLC intake was also significantly higher than FRT, but despite that, the total daily caloric intake was similar among the groups, being proportionally reduced the food intake (**Table 1**).

As shown in **Table 1**, mice drinking FRT or GLC for 30 weeks showed a significant increase in body weight compared to CTRL mice (+31%).

Fasting glycemia was significantly higher both in FRT and in GLC groups compared to CTRL group (**Table 1**). During OGTT **(Fig. 1A)**, the glycemic curves of FRT and GLC mice were markedly moved away from CTRL curve at every time-point after glucose charge. Plasma insulin level was slightly increased in GLC group and in a greater extent in FRT group, with respect to CTRL, without reaching any statistical significance (**Table 1**).

In comparison with CTRL animals, FRT mice showed alterations in plasma lipid profile (**Table 2**) featured by increased levels of TG (+43%), cholesterol (+37%), and LDL (+80%), paralleled by a decrease in NEFA (-24%). GLC mice only showed a trend to dyslipidemia that didn't reach the statistical significance, excepting for HDL level (-16%), and for NEFA level that, conversely to FRT group, was increased (+20%) compared to CTRL.

Fructose and glucose drinking increases liver TG and cholesterol content and induces hepatosteatosis.

Hepatic homogenates of FRT mice showed a marked increase in TG and cholesterol content compared to CTRL (+100% and +50%, respectively). In liver homogenates from GLC mice an increase in cholesterol content similar to FRT was found (+42% of the CTRL value), while the TG level tend to increase compared to CTRL, but remained significantly lower than in FRT group (-60%) (**Fig. 1B**).

Oil red staining of liver sections (**Fig. 1C-E**) highlighted a marked lipid deposition both in FRT (**D**) and in GLC mice (**E**) compared to CTRL (**C**), resembling a condition of non-alcoholic fatty liver disease, with different histopathological features. FRT mice liver showed enlarged hepatocytes with periportal macrovacuolar steatosis. In contrast, liver of GLC mice showed a microvesicular steatosis with a panlobular dissemination. A significantly higher steatosis grade was detected in FRT compared to GLC mice, conferring an overall NAS score of 5.2±1.3 to FRT vs. 3.8±0.9 to GLC mice liver ($P<0.05$) (**Fig. 1F**).

Fructose and glucose drinking enhances TG and cholesterol synthesis through activation of SCAP-SREBP signalling.

To further investigate the greater lipogenic effect of FRT with respect to GLC, we assessed the expression and activation of SREBP1c, SREBP2 and their activating protein SCAP by western blotting analysis **(Fig. 2)**.

SCAP was markedly up-regulated in FRT and GLC mice compared to CTRL (**Fig. 2A,B**), in a significantly greater extent in FRT than in GLC. Both SREBP1c and SREBP2 were up-regulated in

FRT and GLC groups compared to CTRL (**Fig. 2C-H**). Specifically, the 68 kDa active form (**Fig. 2C,E**) and the 125 kDa inactive form (**Fig. 2F,H**) of SREBP1c were significantly more expressed in liver of FRT mice than in GLC. In contrast, SREBP2 was equally activated in FRT and GLC liver (**Fig. 2D,E**), while inactive form of SREBP2 was more expressed in GLC liver than in FRT, without reaching significant difference (**Fig. 2G,H**). The activation of the SCAP/SREBP pathway is confirmed by the increased expression in FRT and GLC mice liver of both the SREBP1c target gene encoding acetyl coenzyme A carboxylase (ACC), one of the enzymes that promote triglyceride synthesis, (**Fig. 3A,B**), and the SREBP2 target gene encoding hydroxymethyl coenzyme A reductase (HMGR), the rate limiting enzyme of the cholesterol synthesis (**Fig. 3C,D**). Notably, the expression of ACC is about 35% greater in FRT than in GLC mice liver (**Fig. 3B**) according to the higher activation of SREBP1c.

ApoB100 protein level was measured in plasma and liver as marker of VLDL secretion (**Fig. 3E**), while the expression of carnitine palmitoyl transferase 1 (CPT1-L) (**Fig. 3G**) indicates the efficiency of β-oxidation. Any significant differences were seen in ApoB100 plasma-to-liver protein level (**Fig. 3F**) and in liver expression of CPT1-L (**Fig. 3H**), among the three groups, although a trend to a reduction of CPT1-L level was seen in GLC mice.

Fructose and glucose drinking enhances AGEs generation and activates RAGE signalling.

As shown in **Table 3**, all AGEs here measured were markedly increased in liver homogenates of FRT and GLC mice compared to CTRL. Most notably, GLAP and MOLD highest levels were detected in the liver of GLC-drinking group, while GOLD and CML were produced in the greatest amount in the liver from FRT group (**Table 3**). The receptor for AGEs, RAGE, was up-regulated both in FRT and GLC mice compared to CTRL (+100%) (**Fig. 4A,B**) and the downstream signalling was activated as demonstrated by the nuclear translocation of NFkB-p65 (**Fig. 4C,D**). As consequence, we found increased levels of the NF-kB-dependent protein ICAM-1 in both sugar-drinking groups (**Fig. 4E,F**), and a slight, but not significant, increase of an early marker of fibrosis,

CTGF (**Fig. 4E,F**), even if morphological signs, as collagen I and IV deposition, were still not detectables (data not shown).

CML colocalizes with SCAP in liver of fructose drinking mice.

Immunofluorescence analysis on liver sections from FRT mice showed a prevalent nuclear localization for SREBP1c **(Fig. 5A,B**), consistent with its activation, and a cytosolic perinuclear localization for SCAP (**Fig. 5D,E**). CML localized mainly in cytosol of hepatocytes (**Fig. 5G,H)**, with a perinuclear distribution similar to SCAP. Interestingly, MGO was detected mainly in the endothelium and at the plasmamembrane of hepatocytes (**Fig. 5J,K**).

Double immunofluorescence studies in liver of FRT group confirmed that CML colocalizes with SCAP in the perinuclear zone of the hepatocytes (**Fig. 6A-F**).

CML modifies SCAP in liver of fructose drinking mice.

Finally, co-immunoprecipitation assay has been performed to evaluate SCAP glycosylation by CML (**Fig. 6G,H**). SCAP was immunoprecipitated with Protein A Sepharose, electrophoresed and blotted on nitrocellulose membrane. Membrane was then exposed to CML antibody, revealing a complex between SCAP and CML in liver of FRT mice.

Discussion

This study clearly demonstrates a significant activation of SCAP/SREBP pathway and the following increase in *de novo* lipogenesis, which were associated to high levels of fructose-derived AGEs in the liver of mice chronically exposed to high fructose intake.

Reducing sugars, as fructose and glucose, react spontaneously with amino groups of proteins to advanced glycation end products (AGEs) (27). Although glucose plays a primary role in the formation of AGEs, it is now known that fructose undergoes the same non-enzymatic glycation reaction at a much faster rate. When fructose assumption with foods or beverages is remarkable, its high reactivity may substantially contribute to the tissue formation of AGEs and lead to cellular alterations and dysfunction (38).

Our study shows for the first time a different pattern of hepatic AGEs between FRT and GLC detected by LC-MS. In detail, FRT generates higher levels of AGEs derived from glyoxal, such as GOLD and CML, while we found more AGEs derived from methylglyoxal, MOLD and GLAP, in GLC mice. These differences may just reflect the dissimilar pathways and rates of FRT and GLC metabolism. Moreover, methylglyoxal is less toxic toward hepatocytes than glyoxal being a better substrate for the carbonyl detoxifying enzymes, while the rate of metabolism of glyoxal by hepatocyte metabolizing enzymes is much faster than for methylglyoxal (39). This could account for the greater accumulation of GOLD and CML in FRT mice.

So far there are limited data directly comparing the effects of fructose and glucose *in vivo* on lipid metabolism, the few existing using very high concentration of sugars for a short time (22,40,42,48), and even less on AGEs generation (1,27).

For this reason, the peculiarities of the present study are the characterization of *in vivo* AGEs generation from fructose and the suggestion of their involvement in the increased hepatic lipid synthesis, in comparison with glucose, through an experimental protocol based on low sugar concentrations given for a long time, mimicking the diffused human habit to daily drink sweetened beverages.

In physiological conditions, the potential sources of TG that contribute to fatty liver development are NEFA coming from the hydrolysis of fatty acids stored in adipose tissue, dietary fatty acids and newly synthesized fatty acids through *de novo* lipogenesis (11). Moreover, an impairment of the lipid β-oxidation rate or of the hepatic triglycerides clearance by VLDL may also lead to hepatic lipid accumulation (46). In the present study FRT drinking mice had lower plasma NEFA than GLC mice, while both the liver expression of CPT-1, the rate limiting enzyme of mitochondrial β-oxidation, and the ratio between plasma and liver levels of ApoB100, the structural component of VLDL, did not differ in FRT and GLC mice. These data indicate for the first time that the *de novo* synthesis is the main pathway responsible for the higher lipid accumulation in liver of FRT mice

with respect to GLC, in which other mechanisms, such as reduction of β-oxidation and higher hydrolysis of adipose fat, may contribute to hepatic steatosis, as previously suggested by other authors (30).

Liver is the main tissue involved in fructose handling and *de novo* lipogenesis (18), and many studies have shown that fructose plays a specific role in the pathogenesis of hepatosteatosis and metabolic syndrome due to differential hepatic fructose metabolism (25,32,33). However, the molecular mechanisms by which high fructose diets induce abnormalities in liver TG metabolism are not fully understood.

It has been observed that a simultaneous induction of glycolitic and lipogenic genes is a salient feature when dietary glucose is replaced with fructose. Indeed, fructose ingestion at high doses increases expression of the genes encoding for lipogenic enzymes via the activation of SREBP1 in the liver (29). Thus, we have analyzed the expression of SREBP1c, SREBP2 and of their chaperone protein SCAP in the liver of FRT and GLC drinking mice.

In our work, chronic exposure to low levels of both FRT and GLC induced the activation of the SCAP/SREBP system. Notably, there was a marked difference in SCAP expression between FRT and GLC mice, being higher in FRT, and this could be crucial for the greater induction of lipogenesis by fructose. Indeed, we observed a significantly higher expression and activation of SREBP1c in liver of FRT versus GLC mice, as confirmed by the resulting higher expression of ACC and by the greater hepatic TG accumulation. On the other hand, SREBP2 is equally hyperactivated in FRT and GLC mice, leading thus to similar expression of HMGR and thereby to similar level of cholesterol in liver. Although SCAP is the common activating protein of both SREBP1c and SREBP2, the existence of unidentified regulatory factors, such as nutritional status or food composition, that determine the fate of the SREBP/SCAP complex by distinguishing between SREBP-1c and SREBP-2 processing, has been supposed (17,37).

Insulin is a well-known inducer of SREBP1c activity and hyperinsulinemia may contribute in hyperactivation of lipogenic pathway (7,8). However, in our experimental model FRT and GLC

mice, even showing altered glucose homeostasis, didn't reach a condition of hyperisulinemia adequate to induce the *de novo* lipogenesis.

We then hypothesized a possible interference of CML on SCAP/SREBP system. Indeed, a direct correlation between AGEs serum level and triglyceride level was found in children and adolescent with Type I diabetes (13). Besides, the generation of CML has been observed during high fat/high sugar diets (20,36) and this has been attributed to lipid peroxidation processes (12). A relationship between intracellular lipid accumulation and increase in CML levels has also been recently demonstrated in an *in vitro* model of steatosis (12). Moreover, CML accumulation in the liver of obese individuals has been involved in hepatosteatosis development (41). This is also supported by a study showing that administration of pyridoxamine, an inhibitor of CML formation, reduces plasma triglyceride and cholesterol on Zucker obese rats (2).

Several studies have indicated that interaction of CML with RAGE causes oxidative stress and activation of NFkB via multiple intracellular signal pathways (5,16). Our results demonstrated that both FRT- and GLC-chronic exposure increased hepatic RAGE expression, and consequently activates NFkB and inflammatory/fibrogenic signaling, at the same level. Therefore, the CML involvement in the higher lipogenesis occurring in FRT mice is not mediated by RAGE binding.

A recent *in vitro* study in cultured mesangial cells highlights a direct causal role for CML in SREBPs activation by interfering with SCAP and thus driving SREBPs factors to elude its negative feedback control (52). The glycosylation of SCAP by Golgi enzymes plays an important role in the cycling of SCAP between the ER and the Golgi (31,51). In physiological conditions, high intracellular concentrations of cholesterol prevent transport of the SCAP-SREBP complex from the ER to the Golgi and downregulate SREBPs activation avoiding intracellular cholesterol and lipids overloading (10). CML administration in mesangial cells disrupted the SCAP-mediated feedback regulation of SREBPs, increasing SCAP gene transcription and protein stability, thereby enhancing the cycling of SCAP between the ER and the Golgi and prolonging SREBPs activation (52). Consistently, our immunofluorescence analysis suggested an interaction between CML and SCAP

which were extensively colocalized in the perinuclear zone of the hepatocytes in FRT mice. The result of coimmunoprecipitation technique further reinforced our hypothesis of a cross-link between CML and SCAP, indicating for the first time that a specific interference of CML in SCAP/SREBP system occurs also *in vivo* and, most notably, could be induced by FRT drinking. However, further experiments with specific CML inhibitors are needed for a conclusive demonstration of the causal role of fructose-derived AGEs in the activation of this specific signaling pathway. Recently, uric acid that generates from fructose metabolism has been suggested as a further mechanism contributing at least in part to the lipogenic effect of fructose feeding (23,24). Uric acid has been shown to induce mitochondrial oxidative stress and accumulation of citrate being the substrate for the *de novo* lipogenesis (23). It is known that oxidative stress is an important element in the glycoxidation process that leads to AGEs accumulation (15) and in some cases a direct positive correlation between uric acid and pentosidine levels has been reported (14,34).

In summary, the present results improve our knowledge on fatty liver development and show an association between high levels of fructose-derived AGEs and activation of *de novo* lipogenesis, thus suggesting more caution in the even wider employment of fructose as added sweetener in foods and beverages.

Grants

This study was supported by a grant of CRT Foundation (2010.1954): “Consuming of sugar-added drinks as risk factor for metabolic diseases: emerging role of fructose” and by MIUR, Fondi ex-60%: “High fructose intake: sweetener or health detrimental?”.

Disclosures

No conflict of interest, financial or otherwise, are declared by the authors.

References

1) Ahmed N, Furth AJ. Failure of common glycation assays to detect glycation by fructose. *Clin Chem* 38(7): 1301-3, 1992.

2) Alderson NL, Chachich ME, Youssef NN, Beattie RJ, Nachtigal M, Thorpe SR, Baynes JW. The AGE inhibitor pyridoxamine inhibits lipemia and development of renal and vascular disease in Zucker obese rats. *Kidney Int* 63(6): 2123-33, 2003.

3) Aragno M, Mastrocola R, Medana C, Restivo F, Catalano MG, Pons N, Danni O, Boccuzzi G. Up-regulation of advanced glycated products receptors in the brain of diabetic rats is prevented by antioxidant treatment. *Endocrinology* 146: 5561-5567, 2005.

4) Bierhaus A, Humpert PM, Morcos M, Wendt T, Chavakis T, Arnold B, Stern DM, Nawroth PP. Understanding RAGE, the receptor for advanced glycation end products. *J Mol Med* 83: 876-86, 2005.

5) Bohlender JM, Franke S, Stein G, Wolf G. Advanced glycation end products and the kidney. *Am J Physiol Renal Physiol* 289: F645-59, 2005.

6) Bray GA. Soft drink consumption and obesity: it is all about fructose. *Curr Opin Lipidol* 21: 51-57, 2010.

7) Brown MS, Goldstein JL. Selective versus total insulin resistance. Cell Metab 7:95–96, 2008.

8) Choi SH, Ginsberg HN. Increased very low density lipoprotein (VLDL) secretion, hepatic steatosis, and insulin resistance. *Trends Endocrinol Metab* 22: 353–363, 2011.

9) Elliott SS, Keim NL, Stern JS, Teff K, Havel PJ. Fructose, weight gain, and the insulin resistance syndrome. *Am J Clin Nutr* 76: 911-22, 2002.

10) Espenshade PJ, Hughes AL. Regulation of sterol synthesis in eukaryotes. *Annu Rev Genet* 41: 401-27, 2007.

11) Ferré P, Foufelle F. Hepatic steatosis: a role for de novo lipogenesis and the transcription factor SREBP-1c. *Diabetes Obes Metab* 2: 83-92, 2010.

12) Gaens KH, Niessen PM, Rensen SS, Buurman WA, Greve JW, Driessen A, Wolfs MG, Hofker MH, Bloemen JG, Dejong CH, Stehouwer CD, Schalkwijk CG. Endogenous formation of Nε-(carboxymethyl)lysine is increased in fatty livers and induces inflammatory markers in an in vitro model of hepatic steatosis. *J Hepatol* 56: 647-55, 2012.

13) Galler A, Müller G, Schinzel R, Kratzsch J, Kiess W, Münch G. Impact of metabolic control and serum lipids on the concentration of advanced glycation end products in the serum of children and adolescents with type 1 diabetes, as determined by fluorescence spectroscopy and nepsilon-(carboxymethyl)lysine ELISA. *Diabetes Care* 26(9):2609-15, 2003.

14) Germanová A, Koucký M, Hájek Z, Parízek A, Zima T, Kalousová M. Soluble receptor for advanced glycation end products in physiological and pathological pregnancy. *Clin Biochem* 43(4-5): 442-6, 2010.

15) Giacco F, Brownlee M. Oxidative stress and diabetic complications. *Circ Res* 107(9): 1058-70, 2010.

16) Goldin A, Beckman JA, Schmidt AM, Creager MA. Advanced glycation end products: sparking the development of diabetic vascular injury. *Circulation* 114: 597-605, 2006.

17) Goldstein JL, Bose-Boyd RA, Brown MS. Protein sensors for membrane sterols. *Cell* 124: 35–46, 2006.

18) Hellerstein MK, Schwarz JM, Neese RA. Regulation of hepatic de novo lipogenesis in humans. *Annu Rev Nutr* 16: 523–557, 1996.

19) Hofmann SM and Tschop MH. Dietary sugars: a fat difference. *J Clin Invest* 119: 1089-1092, 2009.

20) Kanner J. Dietary advanced lipid oxidation endproducts are risk factors to human health. *Mol Nutr Food Res* 51: 1094-101, 2007.

21) Kleiner DE, Brunt EM, Van Natta M, Behling C, Contos MJ, Cummings OW, Ferrell LD, Liu YC, Torbenson MS, Unalp-Arida A, Yeh M, McCullough AJ, Sanyal AJ; Nonalcoholic

Steatohepatitis Clinical Research Network. Design and validation of a histological scoring system for nonalcoholic fatty liver disease. *Hepatology* 41: 1313–1321, 2005.

22) Koo HY, Miyashita M, Cho BH, Nakamura MT. Replacing dietary glucose with fructose increases ChREBP activity and SREBP-1 protein in rat liver nucleus. *Biochem Biophys Res Commun* 390(2): 285-9, 2009.

23) Lanaspa MA, Sanchez-Lozada LG, Choi YJ, Cicerchi C, Kanbay M, Roncal-Jimenez CA, Ishimoto T, Li N, Marek G, Duranay M, Schreiner G, Rodriguez-Iturbe B, Nakagawa T, Kang DH, Sautin YY, Johnson RJ. Uric acid induces hepatic steatosis by generation of mitochondrial oxidative stress: potential role in fructose-dependent and -independent fatty liver. *J Biol Chem* 287(48): 40732-44, 2012.

24) Lanaspa MA, Sanchez-Lozada LG, Cicerchi C, Li N, Roncal-Jimenez CA, Ishimoto T, Le M, Garcia GE, Thomas JB, Rivard CJ, Andres-Hernando A, Hunter B, Schreiner G, Rodriguez-Iturbe B, Sautin YY, Johnson RJ. Uric acid stimulates fructokinase and accelerates fructose metabolism in the development of fatty liver. *PLoS One* 7(10): e47948, 2012.

25) Lim JS, Mietus-Snyder M, Valente A, Schwarz JM, Lustig RH. The role of fructose in the pathogenesis of NAFLD and the metabolic syndrome. *Nat Rev Gastroenterol Hepatol* 7(5): 251-64, 2010.

26) Madero M, Perez-Pozo SE, Jalal D, Johnson RJ, Sanchez-Lozada LG. Dietary fructose and hypertension. *Curr Hypertens Rep* 13: 29–35, 2011.

27) Makita Z, Vlassara H, Cerami A, BucalaR. Immunochemical detection of advanced glycosylation end products in vivo. *J Biol Chem* 267: 5133-8, 1992.

28) Mastrocola R, Guglielmotto M, Medana C, Catalano MG, Cutrupi S, Borghi R, Tamagno E, Boccuzzi G, Aragno M. Dysregulation of SREBP2 induces BACE1 expression. *Neurobiol Dis* 44: 116-24, 2011.

29) Mori T, Kondo H, Hase T, Murase T. Dietary phospholipids ameliorate fructose-induced hepatic lipid and metabolic abnormalities in rats. *J Nutr* 141: 2003-9, 2011.

30) Ngo Sock ET, Lê KA, Ith M, Kreis R, Boesch C, Tappy L. Effects of a short-term overfeeding with fructose or glucose in healthy young males. *Br J Nutr* 103(7): 939-43, 2010.

31) Nohturfft A, Bose-Boyd RA, Scheek S, Goldstein JL, Brown MS. Sterols regulate cycling of SREBP cleavage-activating protein (SCAP) between endoplasmic reticulum and Golgi. *PNAS* 96: 11235–11240, 1999.

32) Nomura K, Yamanouchi T. The role of fructose-enriched diets in mechanisms of nonalcoholic fatty liver disease. *J Nutr Biochem* 23:203-8, 2012.

33) Nseir W, Nassar F, Assy N. Soft drinks consumption and nonalcoholic fatty liver disease. World *J Gastroenterol* 16: 2579-88, 2010.

34) Odetti P, Cosso L, Pronzato MA, Dapino D, Gurreri G. Plasma advanced glycosylation end-products in maintenance haemodialysis patients. *Nephrol Dial Transplant* 10(11): 2110-3, 1995.

35) Ouyang X, Cirillo P, Sautin Y, McCall S, Bruchette JL, Diehl AM, Johnson RJ, Abdelmalek MF. Fructose consumption as a risk factor for non-alcoholic fatty liver disease. *J Hepatol* 48: 993-9, 2008.

36) Ruiz-Ramírez A, Chávez-Salgado M, Peñeda-Flores JA, Zapata E, Masso F, El-Hafidi M. High-sucrose diet increases ROS generation, FFA accumulation, UCP2 level, and proton leak in liver mitochondria. *Am J Physiol Endocrinol Metab* 301: E1198-207, 2011.

37) Sato R, Sterol metabolism and SREBP activation. *Archives of Biochemistry and Biophysics* 501: 177–181, 2010

38) Schalkwijk CG, Stehouwer CD, van Hinsbergh VW. Fructose-mediated non-enzymatic glycation: sweet coupling or bad modification. *Diabetes Metab Res Rev* 20: 369-82, 2004.

39) Shangari N, Poon R, O'Brien PJ. Hepatocyte methylglyoxal (MG) resistance is overcome by inhibiting aldo-keto redictases and glyoxalase I catalysed MG metabolism. *Enzymol Mol Biol Carbonyl Metab* 12: 266-275, 2006.

40) Silbernagel G, Machann J, Unmuth S, Schick F, Stefan N, Häring HU, Fritsche A. Effects of 4-week very-high-fructose/glucose diets on insulin sensitivity, visceral fat and intrahepatic lipids: an exploratory trial. *Br J Nutr* 106(1): 79-86, 2011.

41) Singh R, Barden A, Mori T, Beilin L. Advanced glycation end-products: a review. *Diabetologia* 44: 129-46, 2001.

42) Stanhope KL, Schwarz JM, Keim NL, Griffen SC, Bremer AA, Graham JL, Hatcher B, Cox CL, Dyachenko A, Zhang W, McGahan JP, Seibert A, Krauss RM, Chiu S, Schaefer EJ, Ai M, Otokozawa S, Nakajima K, Nakano T, Beysen C, Hellerstein MK, Berglund L, Havel PJ. Consuming fructose-sweetened, not glucose-sweetened, beverages increases visceral adiposity and lipids and decreases insulin sensitivity in overweight/obese humans. *J Clin Invest* 119: 1322-1334, 2009.

43) Suarez G, Rajaram R, Oronsky AL, Gawinowicz MA. Nonenzymatic glycation of bovine serum albumin by fructose (fructation). Comparison with the Maillard reaction initiated by glucose. *J Biol Chem* 264: 3674-3679, 1989.

44) Takeuchi M, Iwaki M, Takino J, Shirai H, Kawakami M, Bucala R, Yamagishi S. Immunological detection of fructose-derived advanced glycation end-products. *Lab Invest* 90: 1117-27, 2010.

45) Tappy L and Lê KA. Metabolic effects of fructose and the worldwide increase in obesity. *Physiol Rev* 90: 23-46, 2010.

46) Tappy L, Lê KA. Does fructose consumption contribute to non-alcoholic fatty liver disease? *Clin Res Hepatol Gastroenterol* 36(6): 554-60, 2012.

47) Targher G. Non-alcoholic fatty liver disease, the metabolic syndrome and the risk of cardiovascular disease: the plot thickens. *Diabetologia* 51: 444-50, 2008.

48) Teff KL, Grudziak J, Townsend RR, Dunn TN, Grant RW, Adams SH, Keim NL, Cummings BP, Stanhope KL, Havel PJ. Endocrine and metabolic effects of consuming fructose- and

glucose-sweetened beverages with meals in obese men and women: influence of insulin resistance on plasma triglyceride responses. *J Clin Endocrinol Metab* 94(5): 1562-9, 2009.

49) Thornalley PJ, Battah S, Ahmed N, Karachalias N, Agalou S, Babaei-Jadidi R, Dawnay A. Quantitative screening of advanced glycation endproducts in cellular and extracellular proteins by tandem mass spectrometry. *Biochem J* 375: 581-92, 2003.

50) Thuy S, Ladurner R, Volynets V, Wagner S, Strahl S, Königsrainer A, Maier KP, Bischoff SC, Bergheim I. Nonalcoholic fatty liver disease in humans is associated with increased plasma endotoxin and plasminogen activator inhibitor 1 concentrations and with fructose intake. *J Nutr* 138: 1452-5, 2008.

51) Velasco A, Hendricks L, Moremen KW, Tulsiani DR, Touster O, Farquhar MG. Cell type-dependent variations in the subcellular distribution of alpha-mannosidase I and II. *J Cell Biol* 122: 39–51, 1993.

52) Yuan Y, Zhao L, Chen Y, Moorhead JF, Varghese Z, Powis SH, Minogue S, Sun Z, Ruan XZ. Advanced glycation end products (AGEs) increase human mesangial foam cell formation by increasing Golgi SCAP glycosylation in vitro. *Am J Physiol Renal Physiol* 301: F236-43, 2011.

Figure captions

Fig. 1. FRT and GLC drinking affect glycaemic control and liver lipid accumulation. (A) Oral glucose tolerance test performed on 6 hrs fasting mice after 30 weeks of water, FRT or GLC drinking. (B) TG and cholesterol content in mice liver. (C-E) Representative 20x magnification photomicrographs of oil red staining on liver sections from CTRL (C), FRT (D), and GLC (E) mice. (F) Pathological grading in liver sections from CTRL, FRT and GLC mice according to the NAFLD activity score system by Kleiner et al**.** (21). Data are means ± S.D. of 8-10 mice per group. **P*<0.05, ***P*<0.01 vs CTRL; †*P*<0.05 vs FRT.

Fig. 2. Expression analysis on SCAP/SREBP pathway. Western blotting analysis for SCAP (A), nuclear active SREBP1c (C) and SREBP2 (D), cytosolic inactive SREBP1c (F) and SREBP2 (G). (B,E,H) Histograms report densitometric analysis of 6-8 mice per group. **P*<0.05, ***P*<0.01, ****P*<0.005 vs CTRL; †*P*<0.05 vs FRT.

Fig. 3. Expression analysis on markers of synthesis, β-oxidation and secretion of hepatic lipids. Western blotting analysis for ACC (A), HMGR (C), ApoB100 (E) and CPT1-L (G). (B,D,F,H) Histograms report densitometric analysis of 6-8 mice per group. ***P*<0.01, ****P*<0.005 vs CTRL; †*P*<0.05 vs FRT.

Fig. 4. Expression analysis on RAGE/NFkB pathway. Representative western blotting analysis on total liver extracts for RAGE(A), on nuclear and cytosolic liver extracts showing NFkB activation (C), on total liver extracts for ICAM-1 and CTGF (E). (B,D,F) Histograms report densitometric analysis of 6-8 mice per group. **P*<0.05, ***P*<0.01 vs CTRL.

Fig. 5. Liver localization of SREBP1c, SCAP, CML, and MGO. Representative 40x/100x magnification photomicrographs of immunofluorescence analysis for SREBP1c (A,B), SCAP

(D,E), CML (G,I) and MGO (J,K) on 4μm cryostatic liver sections. To assess aspecific staining, negative controls were prepared incubating sections only with secondary antibodies (anti-rabbit: C,F; anti-mouse: I,L).

Fig. 6. CML interaction with SCAP. (A-F) Representative photomicrographs of double immunofluorescence for SCAP/CML. SCAP (A,D) was revealed by red fluorescence and CML (B,E) was revealed by green fluorescence. Colocalization is shown in merged images (C,E). (G) Immunoprecipitation studies on liver extracts. SCAP has been immunoprecipitated (IP) and membranes were incubated (IB) with anti-CML or anti-SCAP antibodies. (H) Histogram represent CML to SCAP band density ratio obtained by densitometric analysis of immunoprecipitation studies performed on 5-6 mice per group. Data are means ± S.D. Statistical significance: *$P<0.05$ vs CTRL; †$P<0.05$ vs FRT.

Table 1. General parameters of mice after 30 weeks drinking water, FRT or GLC. Data are means ± S.D. of 8-10 mice per group. *P<0.05, **P<0.01, ***P<0.005 vs CTRL; †††P<0.005 vs FRT.

	CTRL	FRT	GLC
Drink intake (ml/die)	3.7 ± 0.4	6.5 ± 0.5***	11.4 ± 3.8***†††
Food intake (g/die)	3.8 ± 0.9	2.6 ± 0.6*	2.0 ± 0.9**
Caloric intake (Kcal/die)	11.1 ± 2.8	11.3 ± 1.8	12.4 ± 2.1
Body weight increase (g)	12.4 ± 2.0	16.3 ± 2.5***	16.2 ± 2.4***
Fasting glycemia (mmol/l)	4.7 ± 1.0	7.2 ± 1.5**	7.1 ± 0.9***
Insulinemia (μg/l)	1.27 ± 0.07	2.13 ± 1.02	1.68 ± 1.03

Table 2. Plasma lipid profile of mice after 30 weeks of water, FRT or GLC drinking. Data are means ± S.D. of 8-10 mice per group. *P<0.05, **P<0.01, ***P<0.005 vs CTRL; ††P<0.01 vs FRT.

	CTRL	FRT	GLC
TG (mmol/l)	1.12 ± 0.18	1.60 ± 0.28**	1.34 ± 0.33
Cholesterol (mmol/l)	2.26 ± 0.20	3.10 ± 0.36***	2.68 ± 0.63
HDL (mmol/l)	1.46 ± 0.23	1.31 ± 0.24	1.23 ± 0.12*
LDL (mmol/l)	0.80 ± 0.17	1.44 ± 0.44**	0.95 ± 0.31
NEFA (mg/dl)	12.76 ± 1.58	9.75 ± 2.08**	15.29 ± 3.36*††

Table 3. Advanced glycated end-products evaluated by LC-MS in liver homogenates. Data are means ± S.D. of 8-10 mice per group. *P<0.05, **P<0.01, ***P<0.005 vs CTRL; †P<0.05, ††P<0.01, †††P<0.005 vs FRT.

	CTRL	FRT	GLC
Pentosidine (pg/mg prot)	n.d.	7.02 ± 3.98*	8.69 ± 0.92***
GLAP (ng/mg prot)	n.d.	0.36 ± 0.09*	2.20 ± 0.86*†
GOLD (ng/mg prot)	n.d.	148.1 ± 53.7**	98.5 ± 30.0**
MOLD (ng/mg prot)	n.d.	0.37 ± 0.24*	1.08 ± 0.11***††
CML (ng/mg prot)	0.57 ± 0.09	1.34 ± 0.14***	0.76 ± 0.03*†††

Figure 1.

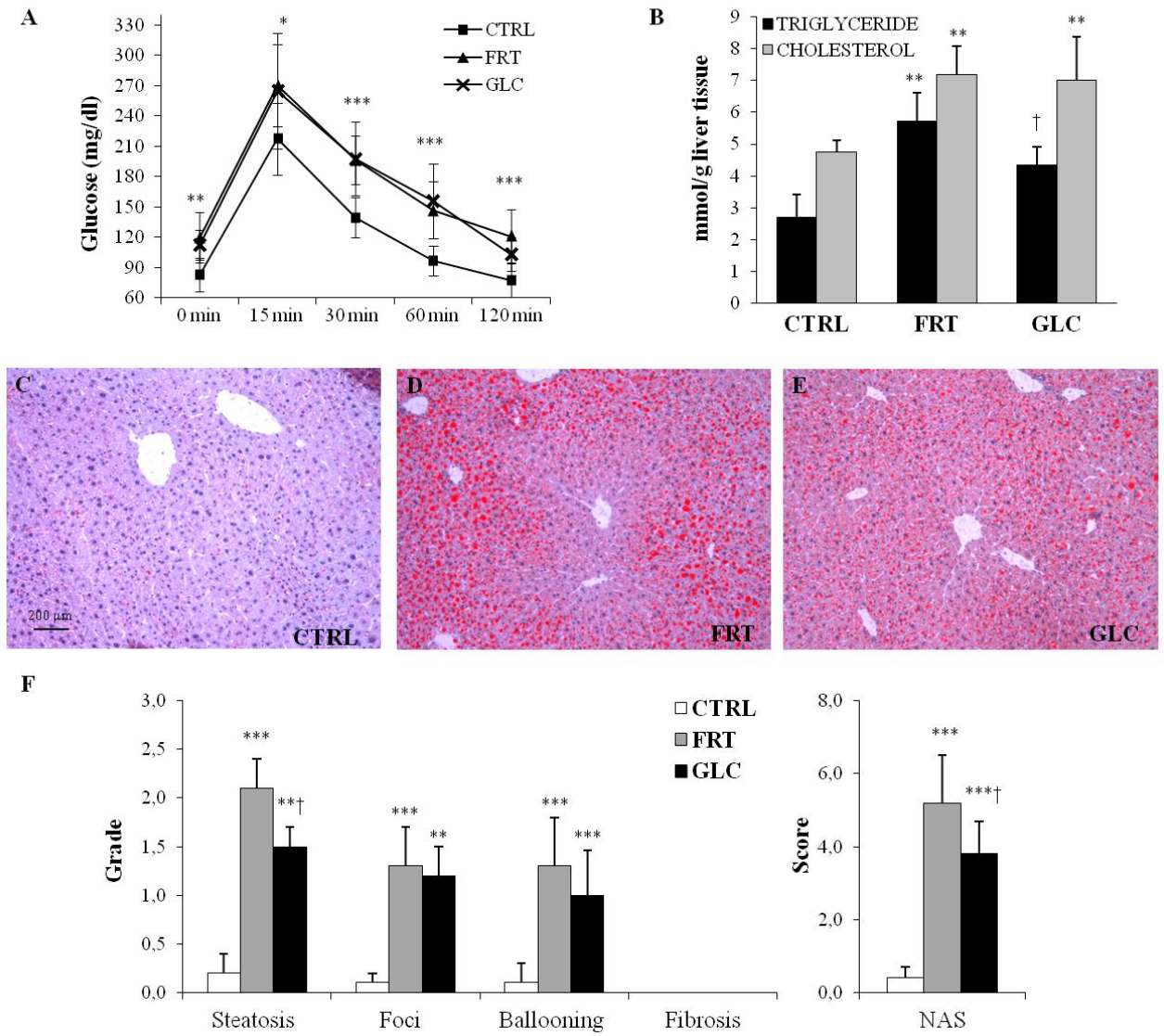
A
Glucose (mg/dl)
330
300
270
240
210
180
150
120
90
60
0 min
15 min
30 min
60 min
120 min
CTRL
FRT
GLC
B
mmol/g liver tissue
TRIGLYCERIDE
CHOLESTEROL
CTRL
FRT
GLC
C
D
E
200 µm
CTRL
FRT
GLC
F
Grade
Steatosis
Foci
Ballooning
Fibrosis
Score
NAS

Figure 2.

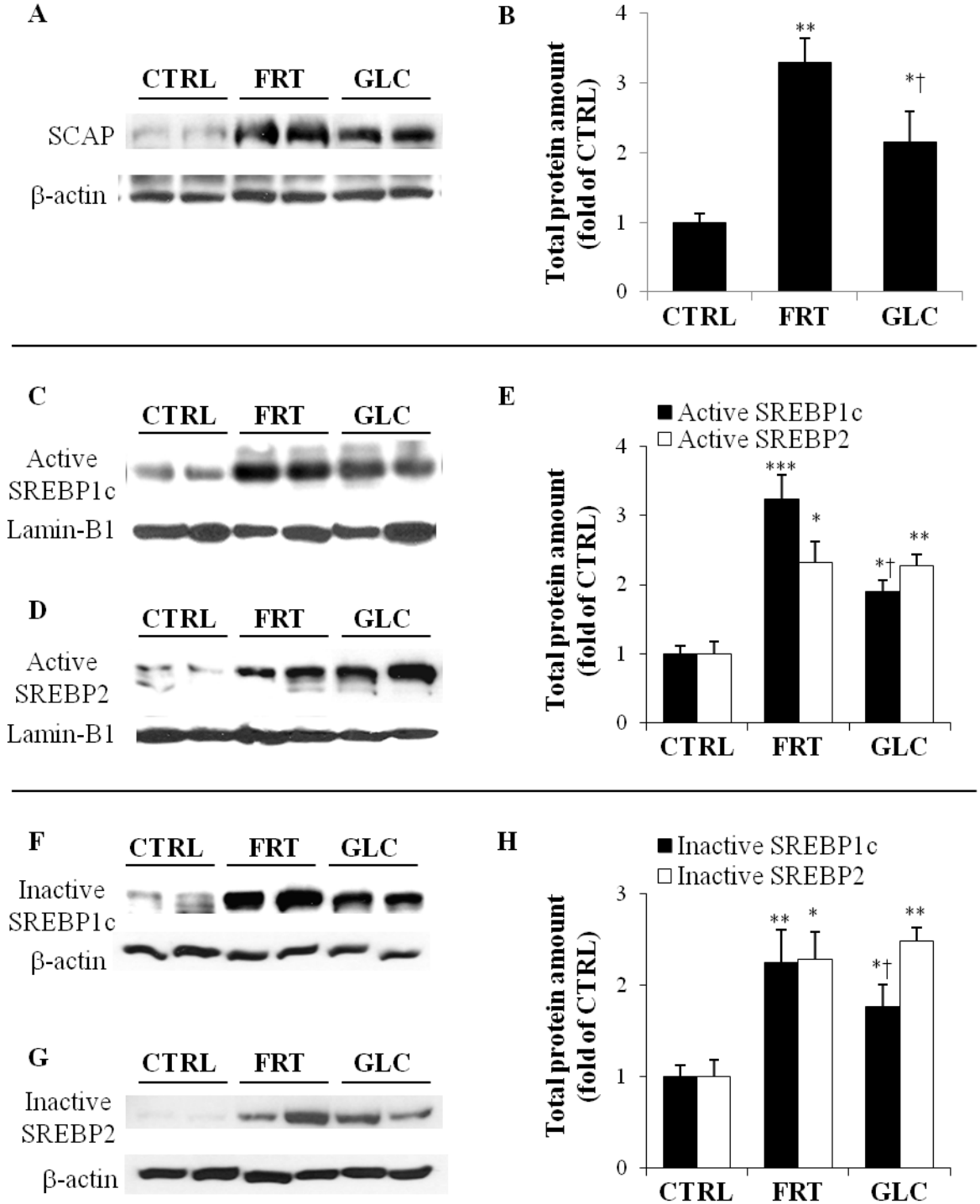
A
CTRL
FRT
GLC
SCAP
β-actin
B
Total protein amount (fold of CTRL)
0
1
2
3
4
**
*†
CTRL
FRT
GLC
C
CTRL
FRT
GLC
Active SREBP1c
Lamin-B1
D
CTRL
FRT
GLC
Active SREBP2
Lamin-B1
E
Active SREBP1c
Active SREBP2
Total protein amount (fold of CTRL)
0
1
2
3
4
***
*
*†
**
CTRL
FRT
GLC
F
CTRL
FRT
GLC
Inactive SREBP1c
β-actin
G
CTRL
FRT
GLC
Inactive SREBP2
β-actin
H
Inactive SREBP1c
Inactive SREBP2
Total protein amount (fold of CTRL)
0
1
2
3
**
*
*†
**
CTRL
FRT
GLC

662

Figure 3.

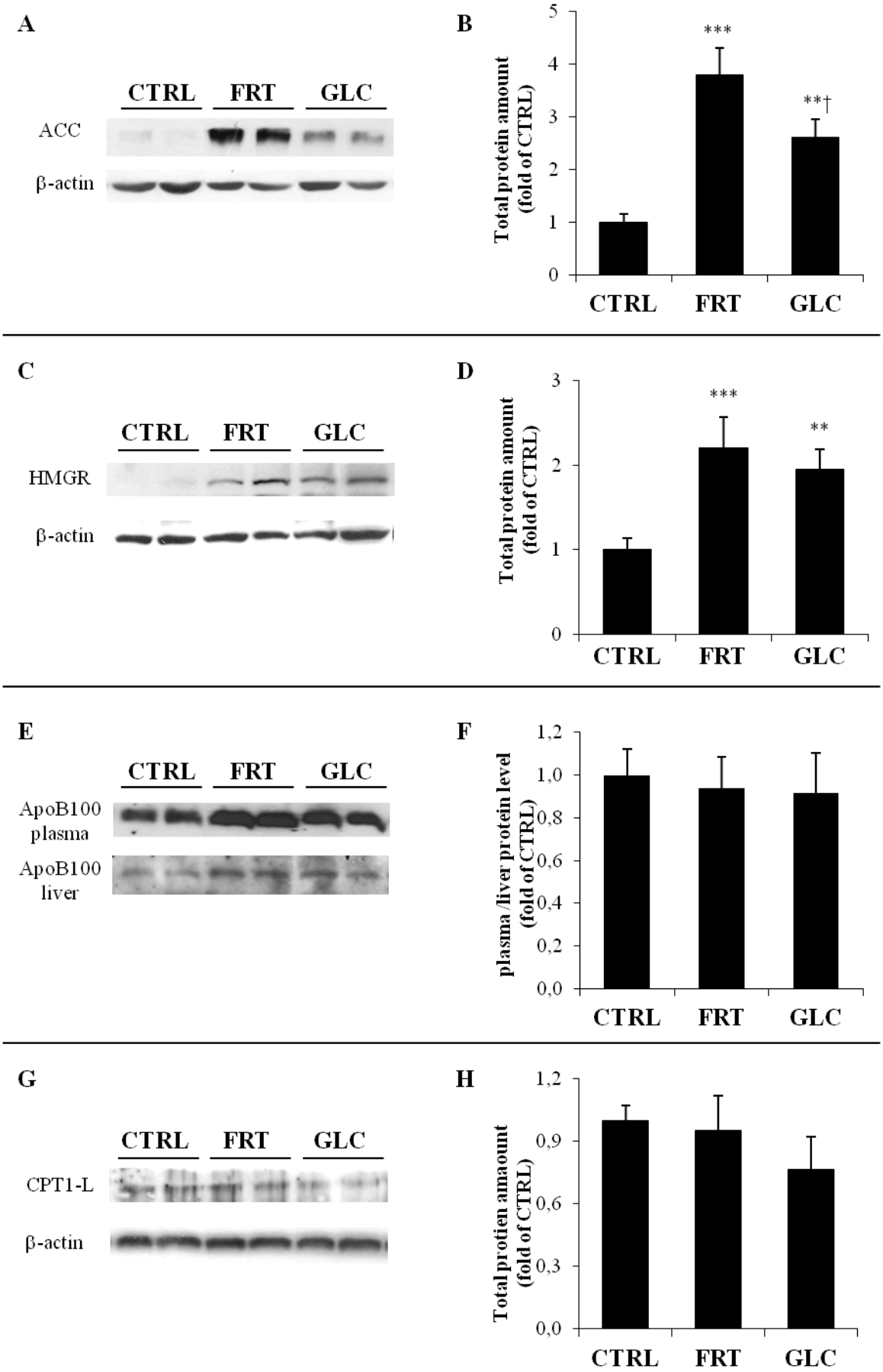
A
CTRL
FRT
GLC
ACC
β-actin
B
Total protein amount (fold of CTRL)
***
**†
CTRL
FRT
GLC
C
CTRL
FRT
GLC
HMGR
β-actin
D
Total protein amount (fold of CTRL)
***
**
CTRL
FRT
GLC
E
CTRL
FRT
GLC
ApoB100 plasma
ApoB100 liver
F
plasma /liver protein level (fold of CTRL)
CTRL
FRT
GLC
G
CTRL
FRT
GLC
CPT1-L
β-actin
H
Total protien amaount (fold of CTRL)
CTRL
FRT
GLC

663

Figure 4.

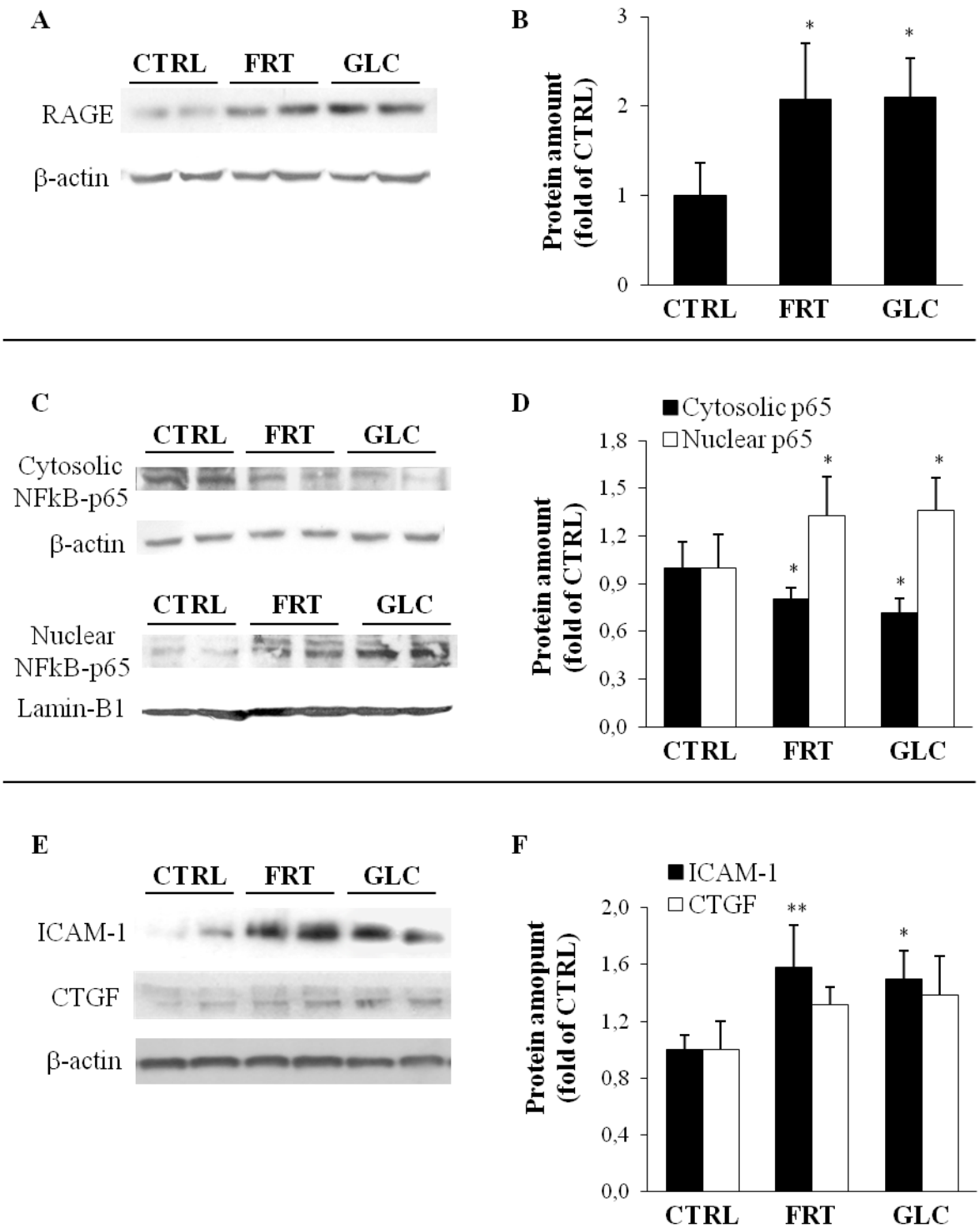
A
CTRL
FRT
GLC
RAGE
β-actin
B
Protein amount (fold of CTRL)
3
2
1
0
*
*
CTRL
FRT
GLC
C
CTRL
FRT
GLC
Cytosolic NFkB-p65
β-actin
CTRL
FRT
GLC
Nuclear NFkB-p65
Lamin-B1
D
Cytosolic p65
Nuclear p65
Protein amount (fold of CTRL)
1,8
1,5
1,2
0,9
0,6
0,3
0,0
*
*
*
*
CTRL
FRT
GLC
E
CTRL
FRT
GLC
ICAM-1
CTGF
β-actin
F
ICAM-1
CTGF
Protein amopunt (fold of CTRL)
2,0
1,6
1,2
0,8
0,4
0,0
**
*
CTRL
FRT
GLC

664

Figure 5.

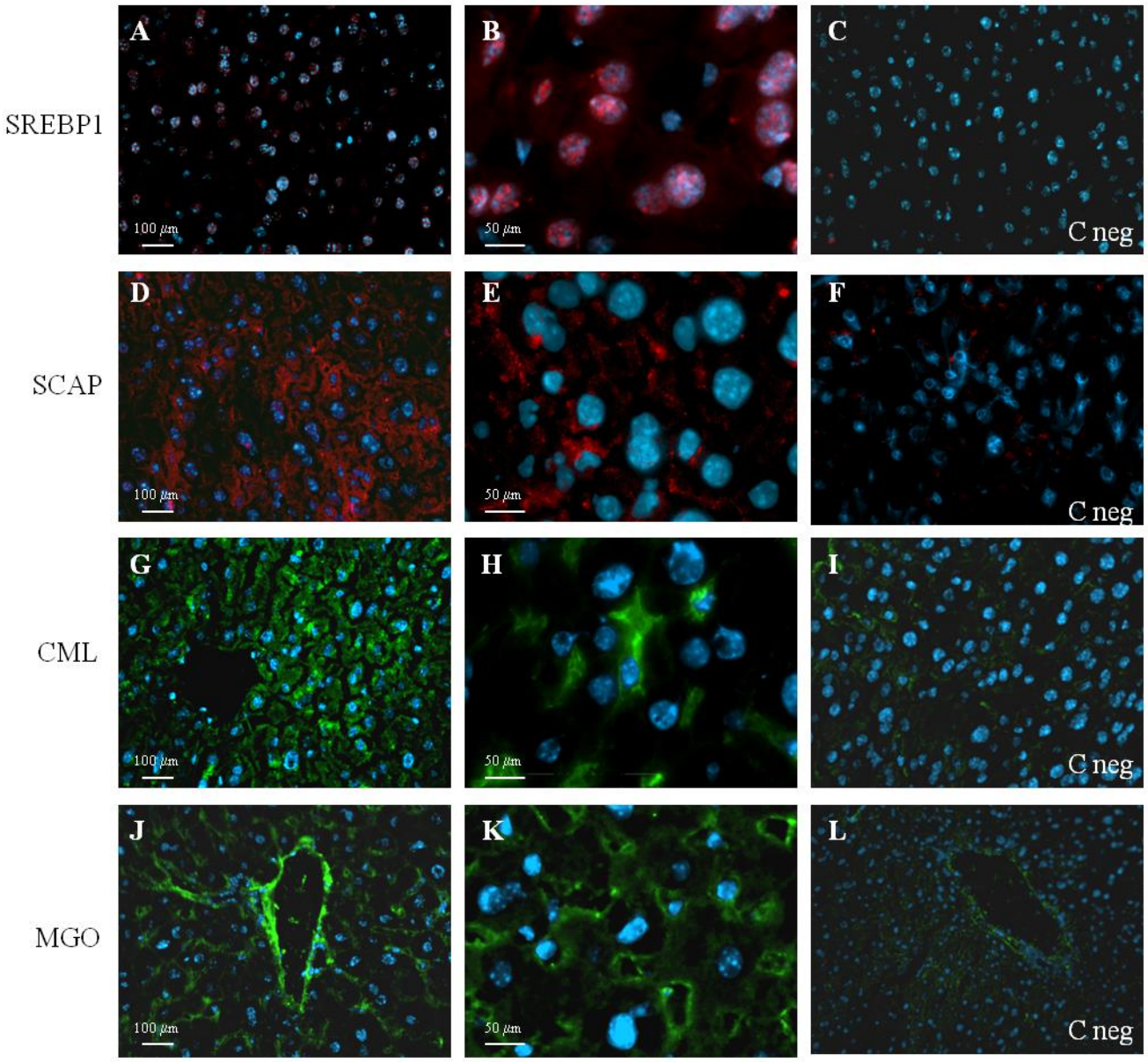

665

Figure 6.

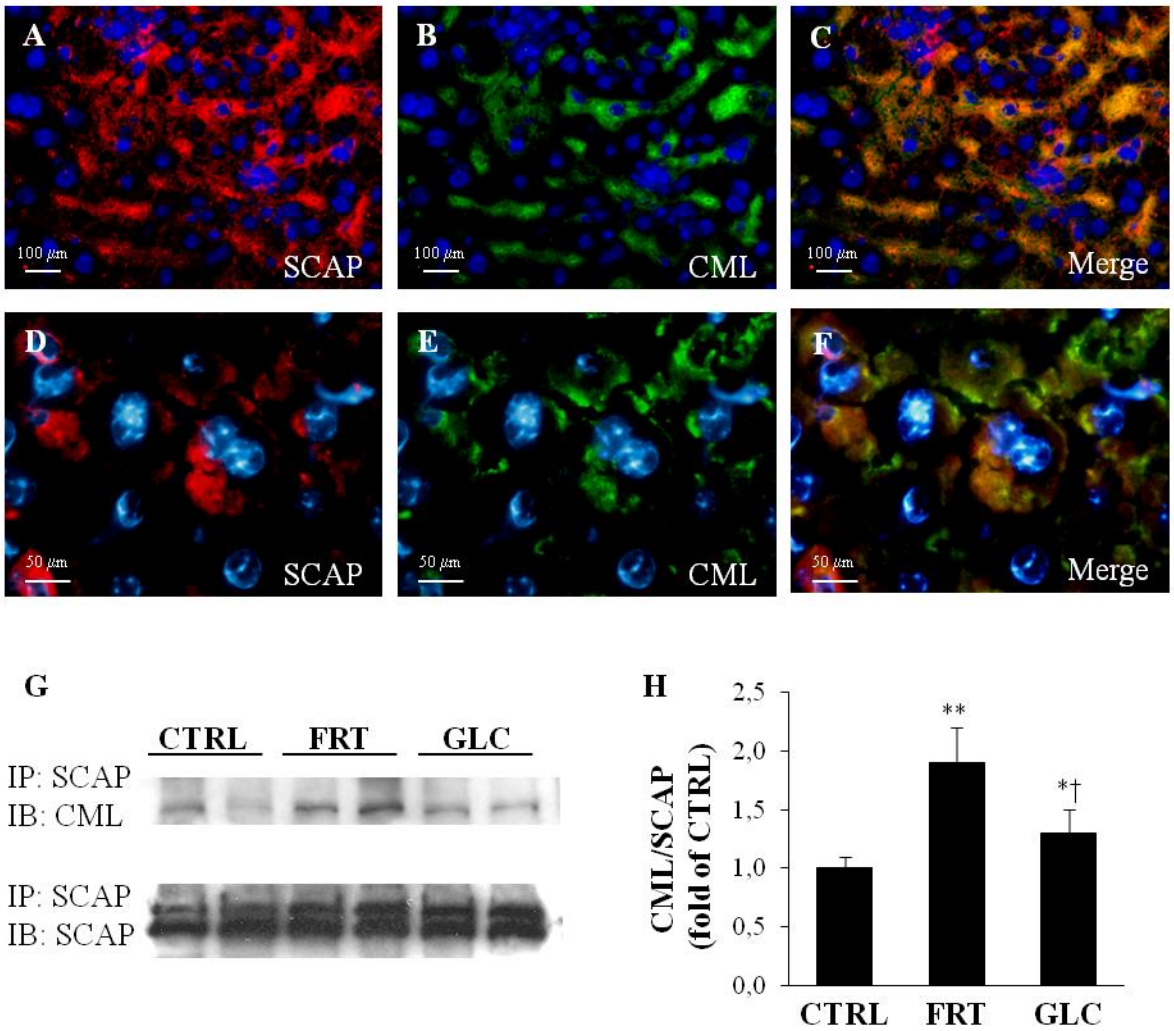
A
100 µm
SCAP
B
100 µm
CML
C
100 µm
Merge
D
50 µm
SCAP
E
50 µm
CML
F
50 µm
Merge
G
CTRL
FRT
GLC
IP: SCAP
IB: CML
IP: SCAP
IB: SCAP
H
CML/SCAP
(fold of CTRL)
2,5
2,0
1,5
1,0
0,5
0,0
**
*†
CTRL
FRT
GLC

666